DOI 10.2478/ama-2024-0028

TESTING THE THERMAL PROPERTIES OF THE INSULATING STRUCTURES OF A FLIGHT DATA RECORDER

Andrzej J. PANAS*, Robert SZCZEPANIAK, Anna KRUPIŃSKA*, Krzysztof ŁĘCZYCKI*, Mirosław NOWAKOWSKI***

*Air Force Institute of Technology, Księcia Bolesława Street No. 6, 01-494 Warszawa, Poland,
**Department of Aviation, Polish Air Force University, Dywizjonu 303 Street No. 35, 08-530 Dęblin, Poland

andrzej.panas@itwl.pl, r.szczepaniak@law.mil.pl, anna.krupinska@itwl.pl
krzysztof.leczycki@itwl.pl, miroslaw.nowakowski@itwl.pl

received 29 March 2023, revised 24 September, accepted 24 September

Abstract: This paper deals with the problems faced during the research on the insulating structures used in the thermal shielding of flight recorders. These structures are characterised by specific properties determined by, among other aspects, their porosity. The complex and coupled heat-exchange phenomena occurring under the operating conditions of the recorders, and in numerous cases combined with mass exchange, require dedicated test methods. The paper characterises the origin of the research problem, presents a methodology for comprehensive testing of the thermal propertiesand uses the example of determining the insulating properties of the Promalight microporous structure ®-1000R. The authors focussed on thermal diffusivity tests performed by means of the oscillatory excitation method. The measurements were conducted on a test stand to determine the effect the type of gas filling had on the porous structure and the pore filling gaspressure effect on the temperature characteristics of apparent thermal diffusivity. The authors also conducted research on the structure's resistance to direct flame exposure. The analysis of the obtained results enable recognition and characterisation of the key phenomena of heat and mass transfer; the numerical results exert a significant influence on their application.

Key words: aerogel insulating structures, thermal–physical properties, thermal diffusivity, Smoluchowski–Knudsen effect, complex thermal analysis, ablation

1. INTRODUCTION

Due to the diversity and stringency of the requirements to be met by flight recorders [6, 10, 14], the very choice of materials for their construction requires a comprehensive approach. For this reason, the evaluation of material properties cannot be limited to the analysis of only selected characteristics, but should take into account all of them along with possible cross-correlations. This includes thermophysical parameters, which by themselves do not characterize the structure holistically. Instead of merely determining properties such as thermal conductivity, heat capacity, etc. special focus should be made on determining properties in the context of the totality of the heat-transfer and the mass-transport phenomena. The very testing procedures and the reliability and representativeness of the obtained results are important aspects here. In fact, the restrictive requirements for the thermal protection of the recorder enforce the use of modern materials rather than material structures. A simple construction and operation problem is becoming a fundamental issue. This problem is underlined by the question whether it is possible at all to describe the properties in terms of the classical parameters of the steady state and unsteady heat-conduction equations [5, 8, 11].

The present paper concerns the study of the fire-resistant microporous structure of Promalight®-1000R [7]. In this case, the complexity of heat-exchange phenomena, the coupling of mechanisms and the possibility of mass-exchange phenomena, for example in the form of phase transformations, determine the need for complex measurements with complementary results to determine individual properties or characteristics. Apart from the appropriate organisation of the overall study [22], in this case, it is essential to maintain as high a temperature resolution as possible [19]. High thermal resolution means that subsequent data points are obtained in such small temperature ranges that the averaging typical for experimental studies does not distort the temperature dependence of the measured parameter. With a low measurement resolution, a distorted image of the temperature characteristics is obtained in the ranges of its non-linearity, which applies, for example, to thermograms in the area of phase transitions. In this case, it is difficult to compare the test data with different parameters at different temperature resolutions. Difficulties also concern the conversion of thermal diffusivity into thermal conductivity, typical for thermophysical research, using the indirect measurement method [12, 13, 19].

According to the requirements of ED 112 norm [6], the recorder should "withstand" the environmental effects of a flame of 1,100 ˚C and a heat flux delivered to the walls of no less than 150 kW·mm^{-2} for at least 20 min in a high-temperature test. In a low-temperature test, the unit is subjected to an ambient temperature of 200 ˚C for 10 h. However, performing a set of measurements over such a large temperature range with all the requirements of complementary testing is extremely difficult. As a whole, however, it is essential to keep the interior with electronic

modules at a temperature not exceeding 130 ˚C. The examined microporous material is being considered in the context of internal insulation. Thus, while developing a test methodology with a different type of thermal protection for the recorders – using phase-change materials – this temperature range was the focus of attention for the research project tasks. The entire study included weight measurements, thermogravimetric (TG), microcalorimetric, i.e. dynamic scanning calorimetry (DSC) and heat diffusion tests by the oscillatory excitation method, as well as tests of the prefabricated product's resistance to a direct flame exposure.

2. MATERIAL STRUCTURES IN EXPERIMENTAL THERMOPHYSICAL RESEARCH

Due to the generally accepted standards for most test methods investigating material properties, also thermo-physical properties, the obtained measurement results are generally reduced to basic defining relationships, such as Fourier's law of heat conduction [26]. This is not entirely correct, for even in the case of a homogeneous solid, the expression of the Fourier–Kirchoff equation

$$\rho\ c_p \frac{\partial\ T}{\partial \tau} \quad = \quad \nabla \cdot \left(\bar{\lambda} \nabla T\right) \ + \ q_V \tag{1}$$

from a theoretical point of view makes it impossible to apply the formula commonly used in experimental practice [5, 21] for the determination of thermal conductivity of form

$$\lambda(T) = \rho(T)\ \ a(T)\ \ c_p(T) \tag{2}$$

While maintaining a high temperature resolution, this approximation is acceptable. However, in the case of heterogeneous materials, there is a problem of determining the resultant properties. For scalar parameters, the homogenisation relationships take form [9]

$$c_p = \sum_i g_i c_{p,i}, \quad \rho = \sum_i r_i \left(\rho_i\right)_{p,T} \tag{3}$$

However, in the case of thermal conductivity only for a steady state and simple parallel or series assembly geometries, the relationship becomes complicated to form:

$$\lambda_{cd,series} \ = \ \left[\sum_i r_i \left(\lambda_{pr,i}\right)^{-1}\right]^{-1} \quad , \quad \lambda_{cd,parallel} = \sum_i r_i \lambda_{pr,i} \tag{4}$$

Geometrically complex systems, including porous structures, require much more complex formulations [2, 23]. In addition, heat transfer phenomena, i.e. convection and radiation, are the rule for porous structures. The following compound formula [5] should be treated with great caution, due to the coupling between mechanisms and the tensor-like general nature of thermal conductivity:

$$\lambda_{apparent} = \lambda_{cd} + \lambda_{cv} + \lambda_r, \qquad \lambda_{cd} = f\left(\lambda_{cd,i},\ r_i; i = 1, \ldots,\ n\right) \tag{5}$$

according to which the contributions of individual phenomena are additive.

The heterogeneity of the structure, its irregularity, the problem of anisotropy and the couplings that cause the behaviour of the physical system to differ from those anticipated by the defining laws do not end the problems. An additional difficulty arises from the need to take into account first-order phase transformation phenomena, which cannot be included as an input to the specific heat. The situation is somewhat bettered by both the statistical scattering of the experimental data the instrumental averaging of results under differential approximations [19]. This provides a basis for interpreting the results of measurements of classical thermo-physical parameters in terms of one of the following relationships:

$$a = \frac{\lambda}{\rho c_p} \quad vs. \quad a(T,p,\ldots) = \frac{\lambda(T,p,\ldots)}{\rho(T,p,\ldots)\ c_p(T,p,\ldots)}$$
$$vs. \quad a(T,p,\ldots) = \frac{\lambda(T,p,\ldots)}{\rho(T,p,\ldots)\left[\frac{\partial h(T,p,\ldots)}{\partial T}\right]_p} \tag{6}$$

However, it is important to emphasize the need for caution-when interpreting experimental data and the need to describe them accurately. In particular, a precise distinction must be made between effective and apparent properties. In analogy to proposals [4, 16], the parameters that are shaped when only one physical mechanism is present should be considered as resultant. Apparent properties refer to the contributions of other processes, e.g. the contribution of convection or radiation to heat transfer with a diffusive description.

Due to the limited framework of this paper, the above methodological considerations do not provide an introduction to an in-depth analysis of the experimental results characterised below. They do, however, justify the need to present the results in an extended form – not only as the final result of a measurement under heat-stabilised conditions, as recommended by many thermal analysis textbooks [25], but also with a description of the process of obtaining the final result.

3. EXPERIMENTAL STUDIES

The concept of comprehensive research includes not only the idea of joint evaluation of the results obtained, but also the interdependence of the measurement procedures (Fig. 1). Maintaining the appropriate order of research and the joint use of data determined at a given stage has both methodological and practical justification. When using the indirect method of determining thermal conductivity [11, 12], it is calculated from the density, specific heat and thermal diffusivity data according to relation (2). From a practical point of view, it is recommended to first conduct microcalorimetric tests and then other measurements with thermogravimetric tests. During the TG test, the thermal resistance of the sample material can be determined, among others, based on the revealed phase-transition temperature or decomposition temperature. This, in turn, allows for the proper determination of the temperature range of the remaining tests. However, it is crucial to be able to jointly evaluate the obtained thermograms to properly determine the properties of the tested material.

Weight, thermogravimetric, microcalorimetric, flame resistance and heat diffusion characterised by effective/apparent thermal diffusivity tests were carried out as part of this project. While investigating the thermal diffusivity two factors shaping the behaviour of the porous structure were taken into account, namely temperature variation and pressure variation of the gas filling the pores. The object of research was the microporous structure of Promalight®-1000R high-temperature insulation. According to the manufacturer [7], it is an opaque glass fibre-reinforced colloidal (pyrogenic) silica blend with an open pore structure. Selected data from the product information sheet are shown in Tab. 1. Based on

data on the effective density of the structure (Tab. 1) and the literature value of the silica density given at 2,650 kg·m^{-3}, the porosity of the material can be estimated at approximately 90%. Samples for testing were prepared from a flat panel, approximately 10 mm thick.

Tab. 1. Material properties of Promalight®-1000R [7]

ρ = 320 kg·m^{-3} (default for RT)				
t (°C)	200	400	600	800
λ (W·m^{-1}·K^{-1})	0.022	0.024	0.029	0.039
c_p (J·g^{-1}·K^{-1})	0.92	1.00	1.04	1.04

RT, room temperature.

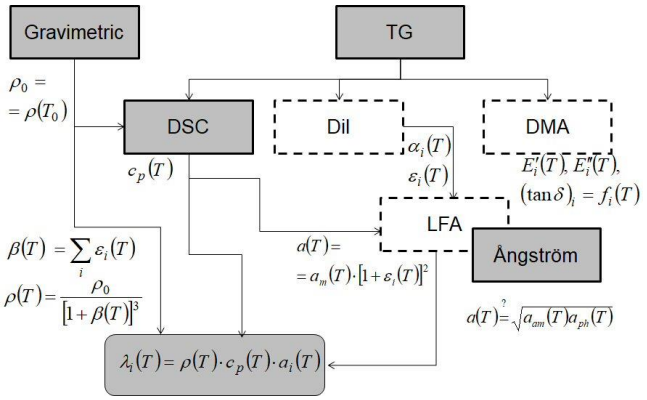

Fig. 1. Schematic diagram of the interdependence of the individual thermo-physical property tests, highlighting measurements not performed (dashed line) as part of the implementation of this project.DMA, dynamic thermomechanical analysis; DSC, differential scanning calorimetry; TG, thermogravimetry

3.1. Flame resistance tests

Due to a high demand for this type of material (which resists degradation during a prolonged operation at elevated temperatures [27, 29, 30]), an attempt was made to determine the effect of flame action on the material structure by measuring the temperature at the rear surface. The samples prepared for testing were cylindrical in shape with a diameter of approximately 50 mm and a thickness of approximately 10 mm. The tests were conducted on a test stand, designed by the authors. The test duration equalled 180 s. The sample was mounted on a fireproof board made of plasterboard. A Ceresit high-temperature filler was used for the gap between the sample and the casing, with a resistance temperature of up to 1,500 °C. J-type thermocouples (t_{s1} – t_{s3}) were used to measure the temperature of the rear surface. The temperature was recorded using National Instruments' SCB (Shielded Comparator Block) instrument and LabVIEW software. The temperature of the ablation surface (exposed to a flame) of the tested sample was measured using a pyrometer (Optris, CT model), along with a head equipped with a laser indicator of the measurement place. For control purposes, the temperature field distribution of the rear surface was also measured using an FLIR i60 thermal imaging camera (t_{th}). Also, a single value of this temperature was read out over a specified period of time. A detailed measurement methodology is presented in Ref.[28].

The obtained result ofthe temperature measurements is given in Fig. 2. The authors also illustrate the distribution of the rear surface temperature field at intervals according to the scale in the picture (Fig. 2). Each measurement made on the rear surface of the sample using the thermal imaging camera is placed at the cross-mark position (Fig. 2) on the temperature diagram and indicated with a red dot (nine measurement points in total). The measurements from the thermocouples indicate a temperature of about 65 °C (for thermocouples) after about 180 s of measurement similar to the thermal camera measurement of 68 °C. The nature of the temperature increase qualitatively is very similar for all readings for both the thermocouples and the measurement from the thermal imaging camera, according to the temperature field distribution in the thermal camera image. Visual inspection of the flame-exposed surface did not reveal any significant damage or loss of sample weight. Only traces of soot were visible on the surface.

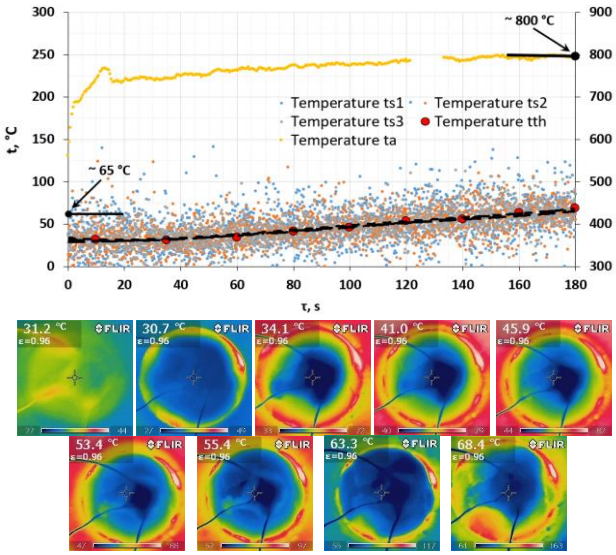

Fig. 2. Diagram with the course of temperature changes on the surface of the tested specimen exposed to the flame (ta – from remote measurements) and on the opposite surface (ts – from thermocouples, tth – IR (infrared) camera), as well as temperature distributions at selected moments on the opposite surface.

3.2. Weight measurements and thermogravimetric analysis

A Mettler Toledo AT 262 analytical balance was used to determine the mass of the test samples. The scale has a resolution of 0.01 mg and a declared accuracy of 0.02 mg. On the basis of the results of weighing control samples of approximately 15 cm^3, the density was determined as 316±10 kg·m^{-3}. The high measurement inaccuracy is mainly due to the measurement error of the thickness of the material panel, which is quite brittle and is subject to the pressure of the measuring tool.

A Netzsch TG 209 F3 Tarsus thermobalance was used to carry out the thermogravimetric tests. The measuring range of the thermobalance covers the temperature range from room temperature (RT) up to 1,000 ˚C, with the resolution equal to 0.1 μg, the maximum weight range of 2,000 mg, the rates of temperature change range from 0.001 ˚ C/min to 100 ˚ C/min and the capacity

of a standard alumina capsule equal to 85 μl. For the measurements, a 14.48 mg sample of crushed material was prepared and pressed with a punch in an open vessel. The first two of the three tests performed immediately one after another were carried out in the range from RT to approximately 130 ˚ C with a declared temperature change rate of 5 K·min^{-1}. The declared rate of change of the temperature of the third measurement up to 550 ˚C was 10 K·min^{-1}. The findings of the TG tests are presented in Fig. 3.

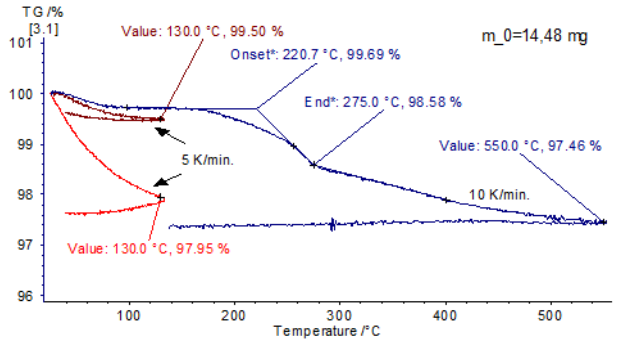

Fig. 3. TG (thermogravimetric) test results – changes in test sample weight as a function of temperature.

The resulting density measurement is consistent with the manufacturer's data. An analysis of the thermograms of the low-temperature TG test shows a likely effect of moisture release. Moisture adsorption in the ambient atmosphere (at room conditions) is typical for porous structures. As the temperature increases in the TG test, water evaporates continuously, which causes a weight loss of several percent. Due to the high enthalpy of water evaporation, even small changes in mass may have significant changes visible in the thermograms of other tests, especially microcalorimetric investigations.This may be reflected in the results of the other tests. High-temperature measurement shows the effect of releasing another component at temperatures >200 ˚C. The type of substance was not identified and the performed differential differential thermogravimetry (DTG) analysis is too inaccurate to determine any other details based on it. However, the indicated onset (beginning of the transformation/decomposition) temperature of 220.7 ˚C indicates the macromolecular nature of the additive.

3.3. Microcalorimetric measurements

DSC i.e. microcalorimetric measurements were performed using a Pyris 1 power-compensated scanning microcalorimeter from Perkin-Elmer with a temperature range of –30 ˚C to 600 ˚C and RT to 710 ˚ C, a declared accuracy of enthalpy and specific heat determination of ± 2% and a capacity of a typical DSC vessel of 25 μl. The three-curve method [12, 13, 15] was used to determine the specific heat, with a proprietary temperature variation programme [18] used in the study. With the latter, it is possible to obtain reliable results of specific heat measurement for both heating and cooling DSC measurement steps – the so-called linear ramps of constant temperature change rate.

As in the previous case, the test sample with an initial mass of 10.17 mg was subjected to several cycles of thermal forcing. A comparison between the results obtained with the first heating cycle and the results obtained in a subsequent measurement, after the sample condition had stabilised, is shown in Fig. 3. An analysis of the results confirms a supposition that moisture absorption has a fairly large effect on material properties, at least on the metrological scale. The increased specific heat values are related to enthalpy changes due to water release. These effects subside with subsequent cycles of thermal forcing. The results of a repeated measurement show more than a satisfactory agreement with the manufacturer's data in the comparative temperature range (>200 ˚ C). They also confirm the transformation effect observed in TG studies at approximately 230 ˚ C.

Direct test results of specific heat are not very suitable for calculation purposes. For the representation of the temperature characteristics and possible conversions, the numerical data were therefore processed using splain function approximation procedures [17]. Splain functions allow the irregularity of the waveforms to be reproduced for essentially any continuity class. The result of the approximation in a graphical form is shown in Fig. 4.

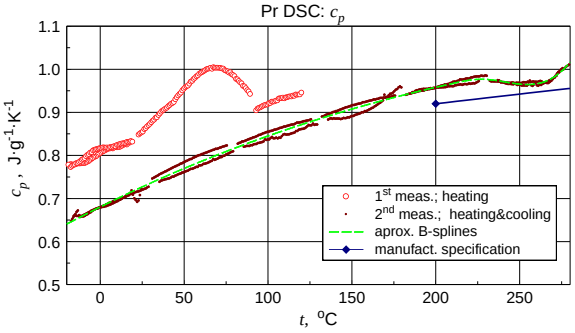

Fig. 4. Results of DSC (differential scanning calorimetry) measurements in the form of specific heat values determined for successive heating segments (measurement 1) or heating and cooling together (measurement 2).

3.4. Heat diffusion tests by temperature oscillation

Both in terms of the applicability of the results and in terms of cognitive aspects, research on heat diffusion is key to the project. Although the oscillatory excitation method used in this research, developed in Ref. [1] and subjected to multiple modifications [3], is to determine the thermal diffusivity and conductivity of the material under investigation, both the scale of the phenomena that can be investigated and the research possibilities are much larger. Particularly when using linear sweep procedures for the temperature range [20], the possibilities for interpreting the resulting signal recordings are greatly expanded. From a metrological point of view, it is also important to be able to achieve a high temperature resolution [19].

The ambient atmosphere test stand and test procedures are described in Ref. [20] where the method modification was presented. The measurement system allows thermal diffusivity to be measured within the range of –30 ˚C to 60 ˚C and of–5 ˚C to 110 °C ,depending on the used coolant and the configuration of the measurement head. In this particular case, the authors used a different test stand, adapted for testing under conditions reduced to technical vacuum and increased to approximately the pressure of 15 bar. This system was developed in connection with the study of thermal phenomena accompanying the absorption of hydrogen by metallic powder deposits [21]. Fig. 5 illustrates a component assembly of the pressure system measuring head. The main

reason for separating the tests between the two systems is the difficulty in separating the effect of temperature changes from the effect of pressure changes in the pressure system.

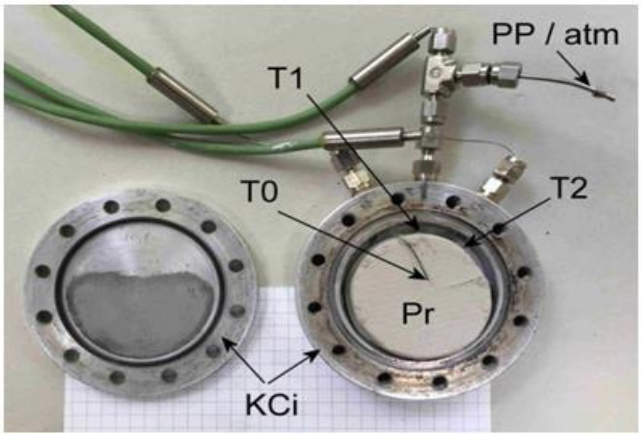

Fig. 5. Photograph of the measuring chamber (KCi) of the pressure system for thermal diffusivity measurement with the test sample (Pr), 0.5 mm K-type sheathed thermocouples (T0, T1, T2) and the marked connection point of the vacuum pump/gas tubes (PP)

The results of the behaviour of the microporous structure under varying temperature conditions with repeated thermal forcing are shown in Figs. 6 and 7. The illustrations contain the determined thermal diffusivity values of the so-called amplitude and phase. For the measurements, a thermal forcing with a period of 60 s or 120 s and an amplitude of about 1 K was used. Due to the limitations of the present study, the authors will limit the characterisation of the differences between these values to the information that the two values should be equal, provided the model conditions are maintained without a heat loss [1, 3, 20].However, it can be emphasised that the Angstrom method is well conditioned metrologically. If there are deviations from the adiabaticity of the sample, the thermal diffusivity value is still between the calculated thermal diffusivity values: amplitude and phase.So, when there are heat losses from the edge of the sample, the actual value under model conditions is included between the higher phase and lower amplitude values [1, 12]. Not only do the boundary heat losses cause the discrepancy in results,they can also be caused by phase transformations not taken into account in the basic model. In the case under consideration, the observed divergence effect is probably due to the release of moisture from the porous structure under investigation. The phenomenon is intensified when the temperature rises. Due to the decreasing vapour pressure and as a result of dehumidification, the effect weakens with a decreasing temperature. It is also observed becoming less intense in subsequent cycles (Fig. 6). Drying the sample stabilises its response to temperature forcing (Fig. 7). The overall results are consistent with the TG and DSC findings.

Clearly, the properties of the porous structure are shaped by the properties of the matrix (the structure's core material) and the filling. The influence of the type and pressure of the filling gas on the determined thermal diffusivity values is illustrated by the test results shown in Figs. 8 and 9. The tests were performed with an oscillation period of 60 s and similar amplitude parameters of the external oscillatory forcing as in the previous case. The gases used for filling, namely helium and dehydrated nitrogen, differ significantly in their thermal conductivity values under standard conditions. The difference reaches one order of magnitude. However, the thermal conductivity as well as other thermodynamic parameters of nitrogen are similar to those of atmospheric air. In order to avoid effects related to moisture sorption, the sample was first degassed and then the temperature level of the oscillation (test temperature) was set to approximately 18 °C. Under these conditions, the discrepancies in amplitude and phase values did not exceed the level featured in Fig. 7 and the geometric mean values of each pair– amplitude value, phase value [1, 20] – were chosen to present the results.

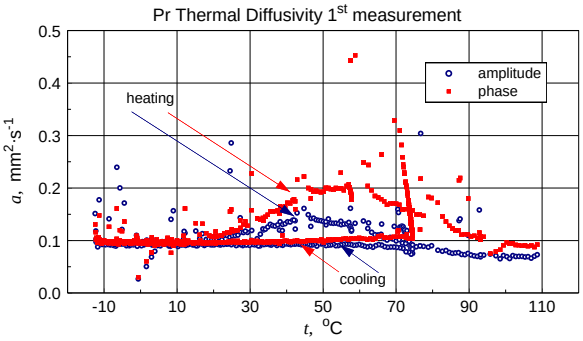

Fig. 6. Amplitude and phase values of the thermal diffusivity of the tested structure as a function of temperature for the first two temperature forcing cycles (open system)

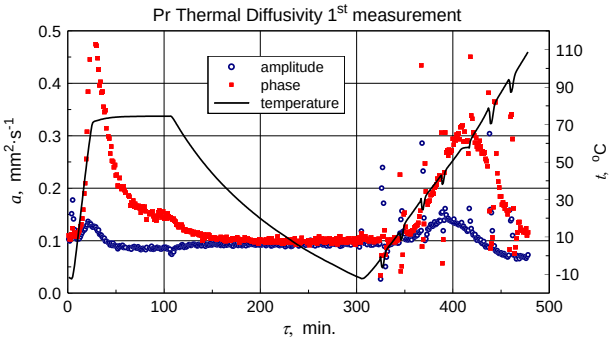

Fig. 7. Results of thermal diffusivity tests during the first temperature forcing cycles in comparison with the force-time characteristics

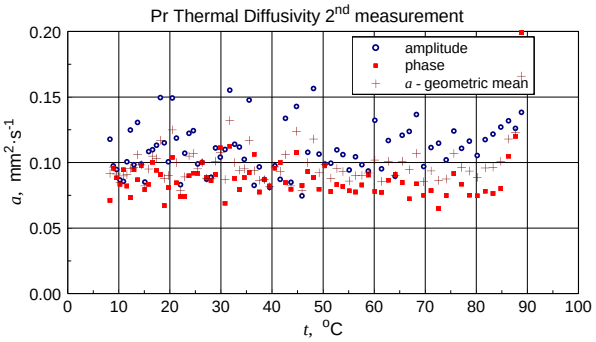

Fig. 8. Effective thermal diffusivity from measurements performed on thermally stabilised specimen – without moisture-releasing effects

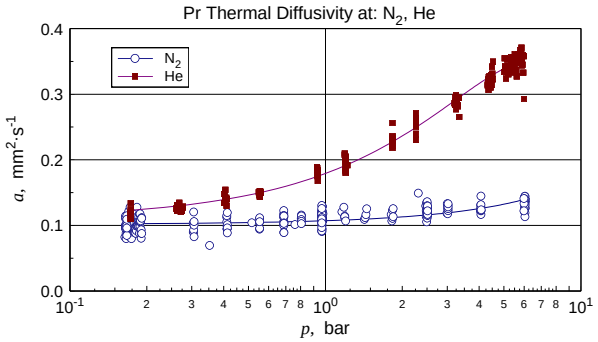

Fig. 9. Geometric mean amplitude and phase values of thermal diffusivity obtained in pressure tests at a constant temperature of approximately 18 ˚C

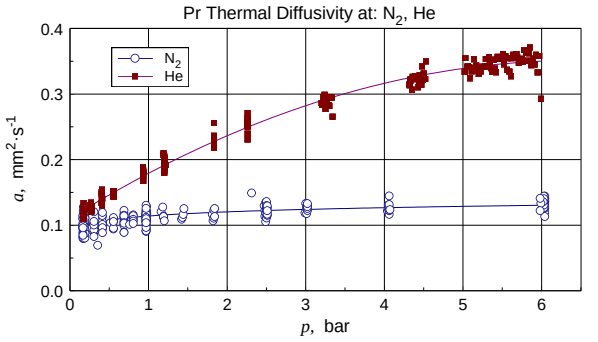

Fig. 10. Representation of test results in the pressure chamber with a logarithmic scale of the abscissa axis

Both figures clearly illustrate both the pressure dependence of the calculated thermal diffusivity values and the quantitative differences for the compared filling gases. At pressures close to normal conditions, the test results for nitrogen filling are consistent with those obtained in an open system for the same reference temperature. With an increase in pressure from approximately 0.15 bar to 6 bar, the calculated diffusivity values for the He filling increased approximately three times and for N2 merely by approximately 40%. It can, therefore, be considered that the conductivity properties of the matrix (base) are similar to those of nitrogen and are far inferior to those of helium. The data illustrated in Fig. 10 show asymptotic convergence with decreasing filling pressures. The relationship can form the basis for an extrapolative determination of the properties of the microporous structure itself. Taking into account the measurement results obtained in an open system, the value of the design diffusivity for this structure can be determined to be approximately 9.5·10–8^{m2}·s^{-1}.

3.5. Analysis of the experimental data

In addition to each individual characterisation of the research results, it is important to emphasise their compatibility. This applies primarily not only to the effects of moisture sorption found with high probability, but also to the irregularity of the thermograms around 230 ˚ C. These phenomena, as well as the results of the influence of the atmosphere filling the open micro pore structure, should be taken into account both when presenting the test results and when developing representative characteristics.

From the point of view of the formation of the properties of the investigated microporous structure, the results of the tests in the pressure chamber are important. In this case, it is worth noting the relationships shown in Fig. 9 in the context of the contribution of gas thermal conductivity, in accordance with relationship [24]

$$\lambda_g = \frac{1}{3}\rho_g \; c_V w \; l \tag{6}$$

which determines the thermal conductivity of the undiluted gas. Since the density of a gas is inversely proportional to pressure and the mean free path is directly proportional to pressure [24],

$$l = \frac{2\mu}{p}\sqrt{\frac{\pi R T}{8}} \tag{7}$$

the thermal conductivity should not depend on the pressure. The thermal conductivity decreases with pressure merely in diluted gases, which is referred to as the Smoluchowski–Knudsen effect. In a porous structure, gas dilution is considered in terms of the ratio of the mean free path to the characteristic dimension of the object, in this case, the dimension of a single pore. In the transitional area, defined by the following Knudsen number values:

$$0{,}1 < \mathrm{Kn} < 10; \quad \mathrm{Kn} = \frac{l}{L} \tag{8}$$

Thermal conductivity values change smoothly and the effect of this can be seen in the results of the thermal diffusivity measurements illustrated in Figs. 8 and 9 in view of relation (2). If the microstructure distribution were characterised by monodispersity, meaning equal pore dimensions, the above relationships canbe used to estimate the characteristic pore dimension. Due to the polydispersity of the examined structure, topological fuzziness is superimposed on the transitional range of the physical model and the issue of evaluating the characteristic dimensions becomes significantly complicated. Nevertheless, one aspect that does not need to be considered is the matter of estimating the minimum distances between the elements of the microstructure. The failure of the design values of thermal diffusivity to stabilise at a constant level along with an increase in pressure means that, for some part of the structure, the investigated heat transport phenomena in the gas phase still remain in the transient range.

As mentioned earlier, great care must be taken when determining representative characteristics, as well as when using the results of heat diffusion tests to determine the resultant or apparent thermal conductivity. However, since the effect of gas density on mass proportions of the homogenisation relationship on cp (3) is negligible, and also the contributions of the gas phase to the resultant density ρ (3) are small, one may attempt to determine representative temperature relationships of the three key parameters characterising transient heat transfer for the thermally non-stabilised state: specific heat, thermal diffusivity and thermal conductivity. The results of the relevant calculations are shown in Tab. 2. To determine the value of the apparent thermal conductivity expressed by relationship (2), a constant density value of 316 kg·m^{-3}, the numerical values of the approximation characteristic of the specific heat (see Fig.4) and the linear regression relationship of mean geometric diffusivity results from Fig. 7 have been used.

Tab. 2. Computational temperature characteristics of the thermophysical properties of the Promalight®-1000R microstructure for the thermally stabilised state

t (°C)	c_p(J·g^{-1}·K^{-1})	a(mm^2·s^{-1})	λ(mW·m^{-1}·K^{-1})
0	0.681	0.0968	20.8
20	0.718	0.0967	21.9
40	0.753	0.0965	23.0
60	0.786	0.0964	23.9
80	0.817	0.0960	24.8
100	0.845	0.0960	25.7
120	0.872	0.0959	26.4

4. CONCLUSIONS

In the light of the detailed conclusions presented in this paper and the results of the development of the measurement data, it is a truism to claim that they all prove the need for comprehensive testing even when attention is focussed on one selected material characteristic. This is because the complementarity of research results allows for proper identification and evaluation of possible off-model phenomena and effects. This is particularly relevant for material structures.

From a methodological point of view, the issue of the correct choice of a method for determining a given property is also important, especially when the property in question cannot be reduced to the category of a real property but is determined in an indirect manner. In this case, it refers to thermal conductivity. It is also necessary to properly present the result of the research, highlighting possible effects conditioned by structural heterogeneity or complexity and coupling of phenomena. In defining representative characteristics, it is appropriate to define the reference condition.

When summarising the test results of the insulating microporous structure of Promalight®-1,000R, it can be concluded that they are largely in line with the manufacturer's declaration (see Tabs. 1 and 2). The research itself, however, provides a pretext for evaluating the used methods and procedures, later exploited for other tasks of the project. It is also interesting to confirm the previously demonstrated capabilities of the oscillatory excitation method and the pressure measurement system [21] for research beyond the strict boundaries of practical applications.

NOMENCLATURE

a	thermal diffusivity (m^2·s^{-1})/(mm^2·s^{-1})		Subscripts
c_p	specific heat (J·g^{-1}·K^{-1})	0	initial state / RT
h	specific enthalpy (J·kg^{-1})	a	front surface temperature
g	mass share (□/%)	am	Amplitude
Kn	Knudsen number	*cd*	conduction
l	average free path (m)	*cv*	convection
L	characteristic dimension (m)	*g*	gas
m	weight (kg)	*i*	component indication
p	pressure (bar)	*p*	constant pressure
q	heat related to unit mass (J·kg^{-1})	ph	phase
r	volume share (●/%)	*r*	radiation
R	individual gas constant (J·g^{-1}·K^{-1})	s1-s3	rear surface temperature from thermocouples
T	temperature (K)	th	rear surface from IR camera
t	temperature (°C)		
u	specific internal energy (J·kg^{-1})		Abbreviations
V	volume (m^3)	Dil	Dilatometry
w	average velocity of the gas molecule (m·s^{-1})	DMA	Dynamic Thermomechanical Analysis
α	linear thermal expansion (K^{-1})	DSC	Differential Scanning Calorimetry
ε	relative expansion i.e. relative length change (□/mm·m^{-1})	DTG	Differential Thermogravimetry
λ	thermal conductivity (W·m^{-1}·K^{-1})	LFA	Laser Flash Analysis
μ	dynamic viscosity (Pa·s)	RT	Room Temperature
ρ	density (kg·m^{-3})	TG	Thermogravimetry
τ	time (s)		

REFERENCES

1. Ångström AJ. Neue Methode, das Warmeleitungsvermogen der Korper zu Bestimmen. Annalen der Physic und Chemie. 1861;114:513-530.
2. Ariaki N, Tang DW, Makino A, Hashimoto M, Sano T. Transient Characteristics of Thermal Conduction in Dispersed Composites. Int JThermophys. 1998;19(1):1239-1251.
3. Belling JM, Unsworth J. Modified Ångström's method for measurement of thermal diffusivity of materials with low conductivity. Rev.Sci. Instrum. 1987;58(6):997-1002
4. Dagan G. Effective, equivalent and apparent properties of heterogeneous media. H. Aref and J.W. Philips (eds.), Mechanics for a New Millenium, Kluwer Academic Publishers, 2001; 473-486
5. Ebert HP, Braxmeier S, Reichenauer G, Hemberger F, Lied F, Weinrich D, Fricke M. Intercomparison of Thermal Conductivity Measurements on a Nanoporous Organic Aerogel. Int. J. Thermophys. 2021;42(21):1-18.
6. EuroCAE ED 112. Minimum operational performance specification for crash protected airborne recorder systems, Revision A September 1. 2013.
7. Etex Industry. Promat Technical Data Sheet. Promalight®. 2022. Available from:www.promat-industry.com
8. Goual MS, Bali A, Quéneudec M. Effective thermal conductivity of clayey aerated concrete in the dry state: experimental results and modeling. J. Phys. D, Applied Physics. 1999;32:3041-3046.
9. Grimvall G. Thermophysical Properties of Materials. Amsterdam: Elsevier Science Publish-ers B.V.; 1986. p.347
10. Jakielaszek Z, Panas AJ, Nowakowski M, Klemba T, Fikus B. Evaluation of numerical modeling application for the crash test planning of the catastrophic Flight Data Recorder. J. Mar. Eng.Technol. 2017;16(4):319-325
11. Kanit T, N'Guyen F, Forest S, Jeulin D, Reed M, Singleton S. Apparent and effective physical properties of heterogenous materials: Representativity of samples of two materials from food industry. Comput Methods Appl Mech Engi, 2006;195:3960 – 3982.
12. Maglić KD, Cezairliyan A, Peletsky VE (Eds.).Compendium of Thermophysical Property Measurement Methods. Volume 1: Survey of Measurement Techniques. New York: Plenum Press. 1984.

13. Maglić KD, Cezairliyan A, Peletsky VE. Compendium of Thermophysical Property Measurement Methods. 1992 Vol. 2: Recommended measurement Techniques and Practices. New York: Plenum Press 1992,
14. NO-16-A200. Wojskowe statki powietrzne, Pokładowe rejestratory katastroficzne, Wymagania i badania [Military aircraft, On-board catastrophic recorders, Requirements and tests] 2006.
15. McNaughton JL, Mortimer CT. Differential Scanning Calorimetry. IRS. Physical Chemistry Series 2 Vol.10. London: Butterworths; Norwalk: reprinted by Perkin-Elmer Corp. 1975; 44.
16. Ostoja-Starzewski M. Mechanics of Random Media. Warszawa: Military University of Technology 2017.
17. Panas AJ. B-spline approximation of DSC data of specific heat of NiAl and NiCr alloys. Arch Thermod. 2003;24:47–65.
18. Panas AJ, Panas D. DSC investigation of binary iron-nickel alloys. High Temp. – High Press 2009;38(1):63-78.
19. Panas AJ. Comparative-Complementary Investigations of Thermophysical Properties – High Thermal Resolution Procedures In Practice. Zmeskal, O. et al. (eds). Thermophysics. Brno University of Technology. Faculty of Chemistry. 2010; 218-235.
20. Panas AJ. IR Support of Thermophysical Property Investigation. Medical and Advanced Technology Materials Study. Prakash, R.V. (Ed.). Infrared Thermography. InTech (Rijeka). 2012;65-90.
21. Panas AJ, Fikus B, Płatek P, Kunce I, Dyjak S, Michalska-Domanska M, Witek K, Kuziora P, Olejarczyk A, Jaroszewicz L, Polański M. Pressurised-cell test stand with oscillating heating for investigation heat transfer phenomena in metal hydride beds. Int. J. Hydrogen Energy. 2016;41:16974-16983.
22. Panas AJ, Błaszczyk J, Dudziński A, Figur K, Foltyńska A, Krupińska A, Nowakowski M. Badania wpływu temperatury na zmiany właściwości cieplnych i mechanicznych osnowy lotniczego konstrukcyjnego materiału kompozytowego. Mechanika w lotnictwie ML-XVII. tom II. Warszawa: PTMTS 2016.
23. Pietrak K, Wiśniewski ST. A review of models for effective thermal conductivity of composite materials. J Pow Technol. 2015;95(1): 14-24.
24. Reif F. Fizyka statystyczna. Warszawa: PWN. 1971; 394.
25. Wendlandt WW. Thermal Analysis. 3rd ed. New York: John Willey & Sons. 1986; 815.
26. Wiśniewski S, Wiśniewski T. Wymiana ciepła. Warszawa:WNT. 2000; 445.
27. Friedrich K, Fakirov S, Zhang Z. Czigány T. Discontinuous basalt fibre-reinforced hybrid composite. Polymer composites: from nano- to macro scale. 2005;309-328.
28. Szczepaniak R, Kozun G, Przybylek P, Komorek A, Krzyzak A, Woroniak G. The effect of the application of a powder additive of a phase change material on the ablative properties of a hybrid composite. Compos Struct. 2021;256:113041. https://doi.org/10.1016/j.compstruct.2020.113041
29. Krzyżak A, Kucharczyk W, Gąska J, Szczepaniak R. Ablative test of composites with epoxy resin and expanded perlite. Compos Struct. 2018;202:978-987. https://doi.org/10.1016/j.compstruct.2018.05.018
30. Przybyłek P, Komorek A, Szczepaniak R. The Influence of Metal Reinforcement upon the Ablative Properties of Multi-Layered Composites.Adv SciTechnol Res J. 2023;17(2).

The work has been accomplished under the research project no. ITWL 36-7401.

Andrzej J. Panas: https://orcid.org/0000-0002-5497-5845
Robert Szczepaniak: https://orcid.org/0000-0003-3838-548X
Anna Krupińska: https://orcid.org/0000-0002-0130-6445
Krzysztof Łęczycki: https://orcid.org//0000-0003-3934-0902
Mirosław Nowakowski: https://orcid.org/0000-0001-6438-5235